The Sad1-UNC-84 homology domain in Mps3 interacts with Mps2 to connect the spindle pole body with the nuclear envelope

Sue L. Jaspersen,[1,2] Adriana E. Martin,[1] Galina Glazko,[1] Thomas H. Giddings Jr.,[2] Garry Morgan,[2] Arcady Mushegian,[1] and Mark Winey[2]

[1]Stowers Institute for Medical Research, Kansas City, MO 64110
[2]Department of Molecular, Cellular, and Developmental Biology, University of Colorado, Boulder, CO 80309

The spindle pole body (SPB) is the sole site of microtubule nucleation in *Saccharomyces cerevisiae;* yet, details of its assembly are poorly understood. Integral membrane proteins including Mps2 anchor the soluble core SPB in the nuclear envelope. Adjacent to the core SPB is a membrane-associated SPB substructure known as the half-bridge, where SPB duplication and microtubule nucleation during G1 occurs. We found that the half-bridge component Mps3 is the budding yeast member of the SUN protein family (Sad1-UNC-84 homology) and provide evidence that it interacts with the Mps2 C terminus to tether the half-bridge to the core SPB. Mutants in the Mps3 SUN domain or Mps2 C terminus have SPB duplication and karyogamy defects that are consistent with the aberrant half-bridge structures we observe cytologically. The interaction between the Mps3 SUN domain and Mps2 C terminus is the first biochemical link known to connect the half-bridge with the core SPB. Association with Mps3 also defines a novel function for Mps2 during SPB duplication.

Introduction

Centrosomes are the primary microtubule-organizing center in most eukaryotic cells. Centrosomes are considered to be soluble cytoplasmic organelles that lack membrane-associated structures. However, centrosomes are closely associated with the nuclear envelope in most interphase cells. A variety of data suggests that a biochemical link exists between the centrosome and nuclear membrane (Bornens, 1977; Nadezhdina et al., 1979; Kuriyama and Borisy, 1981; Malone et al., 2003), and tethering of the centrosome to the nuclear envelope might be important for rapid formation of the mitotic spindle, nuclear positioning within the cell, and/or centrosome inheritance.

SUN (Sad1-UNC-84 homology) domain–containing proteins are an emerging family of inner nuclear envelope proteins that are excellent candidates to play a role in connecting centrosomes with the nuclear envelope. Originally identified based on an ~150-amino-acid region of homology between the C terminus of the *Schizosaccharomyces pombe* Sad1 protein and the *Caenorhabditis elegans* UNC-84 protein (Hagan and Yanagida, 1995; Malone et al., 1999), SUN proteins are present in the proteomes of most eukaryotes (Fig. S2, available at http://www.jcb.org/cgi/content/full/jcb.200601062/DC1; Mans et al., 2004). In addition to the SUN domain, these proteins contain a transmembrane sequence and at least one coiled-coil domain and localize to the inner nuclear envelope. SUN proteins are anchored in the inner nuclear envelope by their transmembrane segment and oriented in the membrane such that the C-terminal SUN domain is located in the space between the inner and outer nuclear membranes. Here, the SUN domain can interact with the C-terminal tail of an outer nuclear envelope protein that binds to the cytoskeleton, including the centrosome (for review see Starr and Fischer, 2005).

The spindle pole body (SPB) is the *Saccharomyces cerevisiae* centrosome-equivalent organelle and is the sole site of microtubule nucleation in budding yeast. The SPB is a multilayered cylindrical structure that is embedded in the nuclear envelope throughout the yeast life cycle (for review see Jaspersen and Winey, 2004). The soluble SPB core consists of

Correspondence to Sue L. Jaspersen: slj@stowers-institute.org

G. Glazko's present address is Department of Biostatistics and Computational Biology, University of Rochester Medical Center, Rochester, NY 14642.

G. Morgan's present address is Institute for Molecular Bioscience, University of Queensland, Brisbane QLD4072, Australia.

Abbreviations used in this paper: 5-FOA, 5-fluoorootic acid; G6PDH, glucose-6-phosphate dehydrogenase; KASH, Klarsicht/ANC-1/Syne homology; MBP, maltose binding protein; SPB, spindle pole body; SUN, Sad1-Unc-84 homology; ts, temperature-sensitive.

The online version of this article contains supplemental material.

The Journal of Cell Biology, Vol. 174, No. 5, August 28, 2006 665–675
http://www.jcb.org/cgi/doi/10.1083/jcb.200601062

three primary layers called the outer, inner, and central plaques. Cytoplasmic and nuclear microtubules are nucleated from the outer and inner plaques, respectively, whereas the central layer of the SPB plays an important role in tethering the organelle to the nuclear envelope. Associated with one side of the core SPB is an electron-dense region of the nuclear envelope termed the half-bridge, which is important for SPB duplication as well as for microtubule nucleation during G1 (Byers and Goetsch, 1974, 1975). SPBs in fission yeast have a similar but not identical structure. Importantly, the *S. pombe* SPB is also embedded in the nuclear envelope, possibly by its SUN protein, Sad1 (Hagan and Yanagida, 1995). Until now, the budding yeast orthologue of Sad1 had not been identified.

The half-bridge is critical for SPB duplication; yet, details of its structure and function at a molecular level are only beginning to emerge. Four proteins are found at the half-bridge: Cdc31, Kar1, Mps3, and Sfi1. Kar1 and Mps3 are integral membrane proteins that localize to the cytoplasmic and nuclear sides of the half-bridge, respectively (Spang et al., 1995; Jaspersen et al., 2002; Nishikawa et al., 2003), whereas Cdc31 and Sfi1 are soluble half-bridge components (Spang et al., 1993; Kilmartin, 2003). Recently, multiple Cdc31 proteins were shown to associate with Sfi1 to form a soluble cytoplasmic filament that spans the length of the half-bridge, and a model in which duplication of the Cdc31-Sfi1 filament generated a non-SPB associated end to initiate assembly of a new SPB was proposed (Li et al., 2006). However, it is unclear how Mps3 and Kar1 associate with this filament and what roles both membrane proteins play during SPB duplication and assembly. One possibility is that Mps3 and Kar1 form the physical half-bridge because mutations in *KAR1* and *MPS3* cause cells to arrest with unduplicated SPBs that lack any recognizable half-bridge structure (Vallen et al., 1994; Jaspersen et al., 2002). Interestingly, Cdc31 and Sfi1 may play a role in the insertion step later in SPB duplication, although this function is poorly understood (Vallen et al., 1994; Kilmartin, 2003). The insertion step of SPB duplication also requires the membrane proteins Mps2 and Ndc1 and their respective binding partners Bbp1 and Nbp1 (Winey et al., 1991, 1993; Schramm et al., 2000; Araki et al., 2006). These proteins may be recruited to the half-bridge to facilitate insertion of the newly formed SPB into the nuclear envelope and/or to tether the half-bridge to the core SPB. Direct binding between the half-bridge and membrane components of the SPB has not been demonstrated, but genetic and two-hybrid interactions between Bbp1 and Kar1 suggest that the half-bridge is connected to the core SPB through these two proteins (Schramm et al., 2000).

Not only is the half-bridge important for SPB duplication, but it is also essential for nuclear migration and fusion after mating (karyogamy; for review see Rose, 1996). During G1, cytoplasmic microtubules are nucleated from the half-bridge instead of from the outer plaque (Byers and Goetsch, 1975). After mating, half-bridge microtubules interdigitate, allowing the two nuclei to congress, and the juxtaposed half-bridges form the site where SPB and nuclear membrane fusion originates (Byers and Goetsch, 1974, 1975). The importance of the SPB half-bridge for nuclear migration and fusion is illustrated by the fact that mutations in *KAR1*, *MPS3*, and *CDC31* cause defects in both steps of karyogamy (Rose and Fink, 1987; Vallen et al., 1994; Nishikawa et al., 2003).

In the present work, we show that budding yeast half-bridge protein Mps3 is homologous to the *S. pombe* SPB component and SUN protein Sad1 (Hagan and Yanagida, 1995). Mps3 also contains a SUN domain, and mutational analysis of this region of Mps3 demonstrated that it is critical for Mps3 function during SPB duplication and karyogamy. The SUN domain of Mps3 binds to the C terminus of another integral membrane component of the SPB, Mps2, and the Mps2–Mps3 interaction is required for formation of an intact SPB. Our results demonstrate at a molecular level how the half-bridge is tethered to the core SPB and describe the consequences of disrupting this interaction. They also support the novel function of SUN proteins in bridging the inner and outer nuclear envelope and provide further evidence that SUN proteins function to tether centrosomes to the nuclear envelope.

Results

MPS3 is related to *SAD1*

MPS3 encodes a 682-amino-acid protein with an acidic N terminus, a transmembrane segment, two coiled-coil domains, and a poly-glutamine region (Jaspersen et al., 2002; Nishikawa et al., 2003). Analysis of secondary structure and local compositional complexity also suggests that the C-terminal region of Mps3 (amino acids 436–682) folds into a discrete globular domain, which has been shown by deletion analysis to be important for Mps3 function (Tables S2 and S3, available at http://www.jcb.org/cgi/content/full/jcb.200601062/DC1; Nishikawa et al., 2003).

To learn more about the function of the C-terminal domain, we searched for similar sequences in protein databases using PSI-BLAST with the model inclusion cutoff set at 0.05 (Altschul et al., 1997). After the first round of search, only Mps3 orthologues from other budding yeasts were detected; however, after the second iteration, we identified numerous proteins from various eukaryotes that showed homology to the Mps3 C terminus. The best matches were to the C-terminal SUN domain of the *S. pombe* Sad1 and to other SUN domain–containing proteins. Alignment of the C terminus of Mps3 with the SUN domain from Sad1 and other SUN proteins indicates a good fit between Mps3 and the sequence consensus of the SUN domain family (Fig. 1 A).

The 514-amino-acid Sad1 protein shares a common overall architecture with Mps3 (Fig. 1 B) and localizes to the SPB (Hagan and Yanagida, 1995), raising the possibility that Mps3 and Sad1 perform similar cellular roles. We overexpressed *SAD1* in various budding yeast temperature-sensitive (ts) mutants in *mps3* and found that growth at the nonpermissive temperature was partially restored in *mps3-ΔSUN2* cells (see the following section; Fig. 1 C), indicating that Sad1 and Mps3 are functionally related.

MPS3 SUN domain mutants

Mutation of the highly conserved asparagine to lysine at position 597 of *MPS3* (Fig. 1 A; N597K) suggests that the SUN domain is important for Mps3 function during mitosis and mating

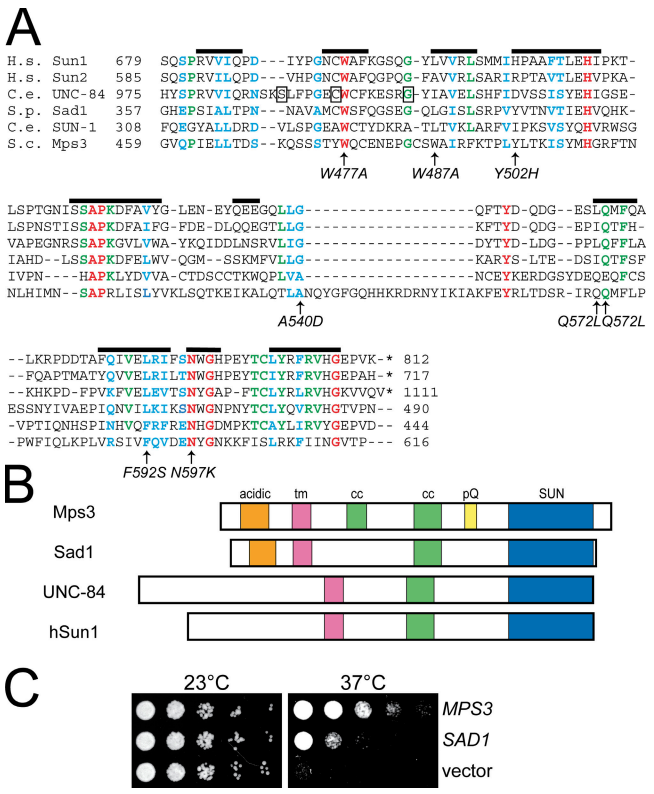

Figure 1. **Mps3 is related to Sad1 and contains a C-terminal SUN domain.** (A) A ClustalW alignment of SUN domains from the indicated proteins shows conserved (red), similar (cyan), and virtually conserved residues (green; in 5 out of 6 SUN proteins included in the alignment). Boxed residues in UNC-84 show the positions of missense mutations that affect nuclear migration (S988F, C994Y, and G1000D), and the arrows show the positions of our ts alleles and a previously described *mps3* mutant, *nep98-7* (N597K; Nishikawa et al., 2003). The predicted β-strands of the SUN domain are shown by bars above the alignment (Mans et al., 2004). (B) Four SUN domain–containing proteins are depicted: *S. cerevisiae* Mps3, *S. pombe* Sad1, *C. elegans* UNC-84, and *H. sapiens* Sun1. All contain at least one transmembrane domain (tm), regions of coiled coil (cc), and a SUN domain. Mps3 and Sad1 also contain an acidic N terminus, but the poly-glutamine region (pQ) is unique to Mps3. (C) *GAL-MPS3*, *GAL-SAD1*, and vector were transformed into the ts *mps3-ΔSUN2* mutant (SLJ1789), and cultures were serially diluted 10-fold and spotted onto plates containing 2% galactose. Plates were incubated at 23 or 37°C for 2 d.

(Nishikawa et al., 2003). To more thoroughly analyze the role of the Mps3 SUN domain, we constructed an allelic series within the Mps3 SUN domain by mutating residues that are conserved or similar in most vertebrate SUN domains (Fig. 1 A) or are conserved in at least four out of the six sequenced *Saccharomyces* species (Cliften et al., 2003). We found that many of the conserved residues are essential for Mps3 function because their mutation results in a nonviable allele (Tables S2 and S3). However, mutation of some conserved residues, such as serine 516, proline 518, and tyrosine 563, had no effect on cell viability. In our analysis, we isolated a series of five new ts *MPS3* alleles (*mps3-W487A*, *-Y502H*, *-A540D*, *-Q572LQ573L*, and *-F592S*; Fig. 1 A and Tables S2 and S3). We also found that loss of the second half of the SUN domain (*mps3-ΔSUN2*; amino acids 524–645) or mutation of the conserved tryptophan at position 477 (*mps3-W477A*) resulted in ts alleles if multiple copies of the mutant gene were present in the cell (Table S3).

The Mps3 SUN domain is required for SPB duplication

We suspected that the SUN domain was critical for Mps3 function during SPB duplication because several of our mutants spontaneously diploidize (Fig. 2, A and B; and Fig. S1, available at http://www.jcb.org/cgi/content/full/jcb.200601062/DC1), a phenotype shared by *mps3-1* and some *kar1* and *cdc31* mutants that are defective in SPB duplication. To test whether our Mps3 SUN domain mutants show defects in SPB duplication, asynchronously growing wild-type and mutant cells were analyzed after a 4-h shift to the nonpermissive temperature (37°C). Flow cytometric analysis of DNA content and budding index confirmed that all of the SUN domain mutants arrest in mitosis at 37°C. Analysis of mitotic spindle morphology by indirect immunofluorescence microscopy and EM revealed that >75% of large-budded *mps3-W487A*, *-Y502H*, *-A540D*, and *-Q572L Q573L* cells contain a monopolar spindle at 37°C (Fig. 2, A and B; and Fig. S1). These results suggest that the SUN domain in Mps3 is required for SPB duplication.

In *mps3-W477A*, *-F592S*, and *-ΔSUN2* mutants, we also observed monopolar spindles in roughly half of the large-budded cells by both indirect immunofluorescence microscopy and EM (Fig. 2, A and B; and Fig. S1). The remaining cells contained short, bipolar spindles with a single DNA mass indicative of a metaphase arrest. This heterogeneous arrest phenotype supports the possibility that Mps3 has a second function in mitotic progression separate from its role in SPB duplication that is defective in these mutants (see Discussion).

Like *mps3-1* mutants, we observed that the growth defect of some of our *mps3* SUN mutants was partially rescued by overexpression of components of the half-bridge, including *CDC31* (Fig. 2 C; Jaspersen et al., 2002). The fact that these mutants also displayed defects in Cdc31 localization at 37°C suggests that their failure in SPB duplication is due to an inability to bind to Cdc31 at the half-bridge (unpublished data). Interestingly, the growth defect of all of the SUN domain mutants at 37°C was suppressed at least in part by overexpression of *NBP1* or *MPS2* (Fig. 2 C). One interpretation of this genetic interaction is that the SUN region of Mps3 might interact directly with Nbp1 or Mps2; therefore, having more of either Mps3 binding partner present in the cell could stabilize a weak interaction with the mps3 SUN mutant protein and allow the *mps3* cells to proliferate at the restrictive temperature. Defects in Cdc31, Mps2, and/or Nbp1 binding could also explain why localization of most of mps3 SUN domain mutant proteins to the SPB is reduced or eliminated in cells grown at 37°C (Fig. 2 E), even though total protein levels determined by Western blotting are not dramatically altered (Fig. 2 D).

mps3 SUN domain mutants have karyogamy defects

Mps3 is important not only for SPB duplication but also for karyogamy. Analysis of the *nep98-7* allele, which contains a mutation in one of the most highly conserved residues in the SUN domain, indicated that Mps3 is required for both steps of karyogamy: nuclear congression and fusion (Nishikawa et al., 2003). To test whether our mutants displayed karyogamy

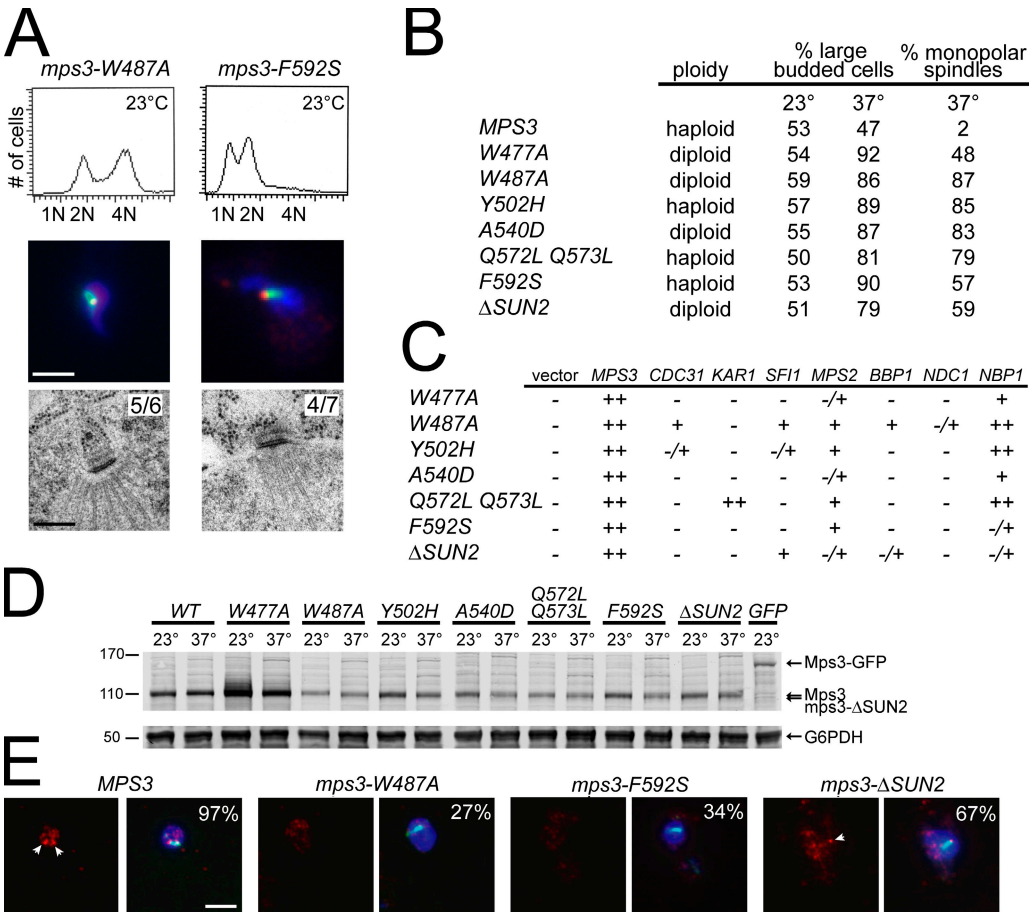

	ploidy	% large budded cells 23°	37°	% monopolar spindles 37°
MPS3	haploid	53	47	2
W477A	diploid	54	92	48
W487A	diploid	59	86	87
Y502H	haploid	57	89	85
A540D	diploid	55	87	83
Q572L Q573L	haploid	50	81	79
F592S	haploid	53	90	57
ΔSUN2	diploid	51	79	59

	vector	*MPS3*	*CDC31*	*KAR1*	*SFI1*	*MPS2*	*BBP1*	*NDC1*	*NBP1*
W477A	-	++	-	-	-	-/+	-	-	+
W487A	-	++	+	-	+	+	+	-/+	++
Y502H	-	++	-/+	-	-/+	+	-	-	++
A540D	-	++	-	-	-	-/+	-	-	+
Q572L Q573L	-	++	-	++	-	+	-	-	++
F592S	-	++	-	-	-	+	-	-	-/+
ΔSUN2	-	++	-	-	+	-/+	-/+	-	-/+

Figure 2. ***mps3* SUN domain mutants are defective in SPB duplication and karyogamy.** (A, top) Flow cytometric analysis of DNA content showed that some *mps3* SUN domain mutant cells (e.g., *mps3-F592S*) are haploids (1N and 2N) at the permissive temperature of 23°C, whereas others (e.g., *mps3-W487A*) spontaneously diploidize (2N and 4N). ts *mps3* SUN domain mutants (Table S1, available at http://www.jcb.org/cgi/content/full/jcb.200601062/DC1) were grown to midlog phase at 23°C and then shifted to 37°C for 4 h. (middle) Indirect immunofluorescence microscopy revealed that both mutants arrest at 37°C with monopolar spindles: a single microtubule array (anti-Tub1; green) nucleated from one SPB (anti-Tub4; red) associated with one DNA mass (DAPI; blue). Bar, 5 μm. (bottom) Nuclei from large budded cells were examined by EM to further examine SPB number and mitotic spindle structure. Thin section images of representative SPBs, the number cells with the depicted SPB number/structure, and the total number of nuclei examined is shown. Bar, 0.2 μm. (B) The experiment in A was performed with other *mps3* SUN domain mutants (Fig. S1). The DNA content of each mutant at 23°C, the percentage of large-budded cells for each sample at 23°C and 37°C, and the percentage of large-budded cells with monopolar spindles at 37°C was determined ($n = 200$ in three independent experiments). (C) The indicated gene on a 2μ *URA3* plasmid (pRS202 or pRS426) was transformed into each *mps3* SUN mutant and analyzed for its ability to restore growth at 37°C in a serial dilution assay. 2 OD_{600} of cells from an overnight culture were spotted onto SD-URA plates in a series of six fivefold dilutions. After 3 d at 37°C, suppression was scored as follows: ++, growth at the fourth dilution and beyond; +, growth at the second or third dilution; −/+, growth only at the first dilution; −, no growth above background. None of the mutants were suppressed by 2μ *SPC42*, 2μ *SPC29*, 2μ *CNM67*, or 2μ *NUD1* (not depicted). (D) Levels of wild-type Mps3 or mps3 mutant proteins in cell extracts from A and B were determined by Western blotting with anti-Mps3 antibodies (top). We also included a sample from a strain in which the endogenous copy of *MPS3* was replaced with *MPS3-GFP* (GFP; SLJ911); because Mps3-GFP is 27 kD larger than wild-type Mps3, this allows us to clearly determine the position of endogenous Mps3. G6PDH serves as a loading control (bottom). (E) In the same cells grown at 37°C, localization of wild-type Mps3 and mutant mps3 proteins to the SPB, marked by the end of the microtubule signal, was analyzed by indirect immunofluorescence microscopy with affinity-purified Mps3 polyclonal antibodies. Anti-Mps3 is in red, microtubules are in green, and DNA is in blue. Arrowheads point to SPB-localized Mps3, and the percentage of cells with visible Mps3 at the SPB is indicated ($n = 100$ in two independent experiments). In addition to what is shown, 38% of mps3-W477A, 58% of mps3-Y502H, 11% of mps3-A540D, and 17% of mps3-Q572L Q573L protein localized to the SPB at the SPB at 37°C; in the remainder of cells, a diffuse staining pattern similar to that of mps3-W487A and mps3-F592S was observed. All of the mutant mps3 proteins localized to the SPB in >80% of cells at 23°C (not depicted). Background staining away from the SPB is due to a combination of Mps3 localization to the nuclear periphery (Jaspersen et al., 2002; Nishikawa et al., 2003) as well as nonspecific cross-reactivity of the antibody; therefore, only Mps3 localization to the spindle poles was analyzed. Bar, 5 μm.

defects, we analyzed the position of nuclei in mating mixtures of wild-type and *mps3* SUN domain mutants after 5 h at the semipermissive temperature of 30°C; at higher temperatures, karyogamy itself is affected and our mutants begin to exhibit a significant delay in mitosis, a cell cycle stage that is nonpermissive for mating. After 5 h, 95% of zygotes contained a single nucleus in the wild-type mating, whereas only 60–70% of *mps3* SUN domain mutant zygotes had successfully completed both steps of karyogamy and contained a single nucleus (Fig. 3). The SUN domain mutants displayed a unilateral defect in karyogamy (unpublished data) and were defective in both nuclear congression and fusion, although the congression defect was more pronounced. We suspect that allele and strain-background differences are responsible for the less severe karyogamy phenotypes that we observed compared with others (Nishikawa et al., 2003). The simplest interpretation of the karyogamy defect, like

mating	genotype	% of zygotes Kar+	congression-	fusion-
SLJ1779 x SLJ1780	*MPS3 x MPS3*	95	4	1
SLJ1793 x SLJ1794	*W477A x W477A*	70	23	7
SLJ1785 x SLJ1786	*W487A x W487A*	63	27	10
SLJ1781 x SLJ1782	*Y502H x Y502H*	70	22	8
SLJ1787 x SLJ1788	*A540D x A540D*	67	26	7
SLJ1783 x SLJ1784	*Q572L Q573L x Q572L Q573L*	65	25	10
SLJ1791 x SLJ1792	*F592S x F592S*	61	27	12
SLJ1789 x SLJ1790	*ΔSUN2 x ΔSUN2*	69	20	11
W303a x W303α	*MPS2 x MPS2*	93	5	2
SLJ2006 x SLJ2007	*mps2-381 x mps2-381*	68	22	10
SLJ717 x SLJ718	*mps2-1 x mps2-1*	85	10	5

Figure 3. **Mutants in the *MPS3* SUN domain and in *MPS2* exhibit karyogamy defects.** Cells from log phase cultures of the indicated mutants were mated at the semipermissive temperature of 30°C for 5 h, and then mating mixtures were stained with DAPI and the position of nuclei in zygotes was observed by fluorescence microscopy. Numbers represent the mean percentage of zygotes with a single mass of DNA (Kar+), two separated masses of DNA (congression−), and two masses of DNA separated by <2 μm (fusion−). 100 zygotes in four independent mating experiments were analyzed.

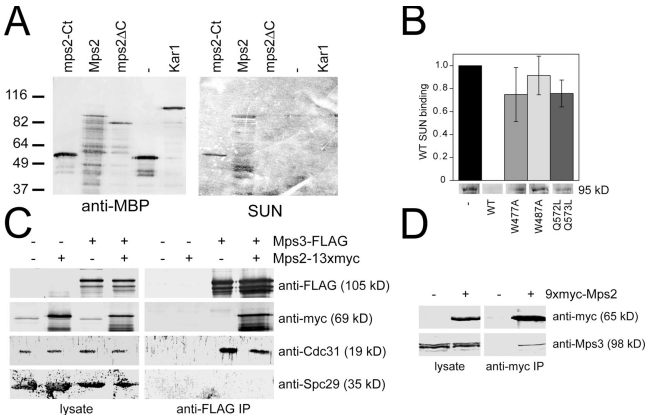

Figure 4. **The Mps3 SUN domain binds to Mps2.** (A) Bacterial extracts from cells expressing MBP (−), MBP-Mps2, MBP-mps2ΔC (amino acids 1–328), MBP-mps2-Ct (amino acids 328–387), and MBP-Kar1 were electrophoretically separated, and proteins were transferred to nitrocellulose membranes. Expression of MBP and the MBP fusion proteins was detected by Western blotting with anti-MBP antibodies (left). Membranes were also probed with 10 μg purified 6xHis-mps3SUN labeled with Alexa 680 in a gel overlay assay (right). (B) Nitrocellulose membranes with MBP-Mps2 were probed at 30°C with 10 μg purified 6xHis-mps3SUN (amino acids 457–617) labeled with Alexa 680 in the presence of nothing (−), 100 μg purified, unlabeled 6xHis-mps3SUN or purified, unlabeled 6xHis-mps3SUN mutants. The decrease in labeled 6xHis-mps3SUN signal was quantitated, and the signals in the presence of no competitor (−) or in the presence of the wild-type SUN domain were assigned values of 1 and 0, respectively. Mean values obtained from three independent experiments are shown. (C) Spheroplast lysates were prepared from wild-type (SLJ001), *MPS2-13xMYC* (SLJ1896), *MPS3-3xFLAG* (SLJ1898), and *MPS2-13xMYC MPS3-3xFLAG* (SLJ1900) strains, and the protein composition of the lysate (left) and the indicated immunoprecipitate (right) was analyzed by Western blotting with anti-MYC, anti-FLAG, anti-Cdc31, and anti-Spc29 antibodies. (D) Liquid nitrogen ground lysates were prepared from wild-type (SLJ001) and *9xMYC-MPS2* (SLJ1996) strains as described in Materials and methods. The protein composition of the lysate (left) and the anti-MYC immunoprecipitates (right) were analyzed by Western blotting with anti-MYC and anti-Mps3 antibodies.

the SPB duplication defect, is that *mps3* SUN domain mutants fail to form an intact half-bridge, which is critical for both nuclear congression and fusion (Byers and Goetsch, 1975).

The Mps3 SUN domain interacts with Mps2

Because Mps3 is located at the SPB and SUN proteins are thought to interact with other integral membrane proteins, we hypothesized that the Mps3 SUN domain might bind Kar1 or Mps2, the other single pass membrane proteins at the SPB (Vallen et al., 1992; Spang et al., 1995; Munoz-Centeno et al., 1999). Full-length Kar1 and Mps2 expressed as maltose binding protein (MBP) fusions in bacteria were transferred to nitrocellulose membranes after SDS-PAGE of bacterial extracts, and the membrane was probed with the Mps3 SUN domain (amino acids 457–617) labeled with the infrared dye Alexa 680 in a gel overlay assay. We found that the SUN domain bound to full-length Mps2 (MBP-Mps2) and to the Mps2 C terminus (MBP-mps3-Ct) but did not interact with MBP, Kar1 (MBP-Kar1), or other proteins in the bacterial extracts (Fig. 4 A). Binding of the Mps3 SUN domain to Mps2 required a functional SUN domain because most mps3 SUN domain mutant proteins were unable to compete with the wild-type protein for Mps2 binding in the gel overlay assay, even when present in at least 10-fold excess (Fig. 4 B and not depicted).

To test whether Mps2 and Mps3 interact in yeast, we created strains expressing *MPS2-13xMYC* and/or *MPS3-3xFLAG* from their endogenous promoters and immunoprecipitated the tagged proteins from the membrane fraction of lysates from spheroplasted cells treated with the short 12-Å membrane-permeable cross-linker dithiobis(succinimidyl)propionate. Mps2-13xMYC coimmunoprecipitated with Mps3-3xFLAG, as did the Mps3 binding protein Cdc31 (Fig. 4 C; Jaspersen et al., 2002). The fact that Mps2-13xMYC did not precipitate in cells lacking Mps3-3xFLAG and that other SPB components such as Spc29 did not coprecipitate indicates that binding is specific and likely occurs through Mps3. Mps2 and Mps3 also coimmunoprecipitated in the absence of a cross-linker when cell lysates were prepared by grinding in liquid nitrogen (Fig. 4 D), providing further evidence of a direct interaction between Mps2 and Mps3 in yeast. However, as SPBs remain largely intact by this method of lysis (Niepel et al., 2005), we cannot totally exclude the possibility that the Mps2–Mps3 interaction is mediated by another SPB component. From the binding data in vitro and our ability to coimmunoprecipitate Mps2 and Mps3 from yeast extracts using two different techniques, we conclude that Mps2 binds to Mps3 in vivo and that this interaction is likely mediated by the Mps3 SUN domain.

The C terminus of Mps2 binds to the Mps3 SUN domain

Several proteins predicted to bind to SUN domains contain a conserved C-terminal transmembrane segment followed by ~30 amino acids known as the Klarsicht/ANC-1/Syne homology (KASH) domain (Starr and Fischer, 2005). Protease protection and protein binding experiments demonstrated that the N terminus of Mps3 is exposed to the cytoplasm/nucleoplasm, whereas the C terminus, including the SUN domain, is located in the space between the inner and outer nuclear membranes

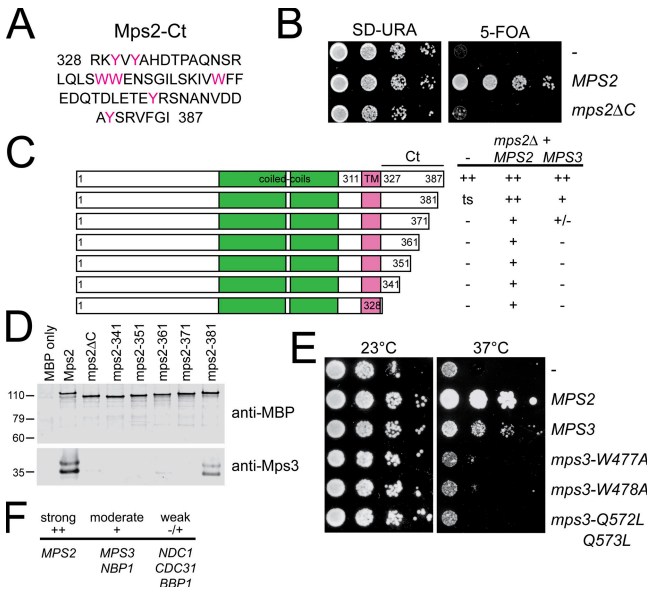

Figure 5. **The C terminus of Mps2 interacts with the Mps3 SUN domain.** (A) Shown is the C-terminal sequence of Mps2 after the transmembrane domain (amino acids 328–387). Aromatic amino acids are shown in magenta. (B) A nonsense codon was inserted after the sequence encoding the transmembrane domain in *MPS2* (codon 328) to generate an allele that lacked the C-terminal domain. This allele, *mps2ΔC*, a wild-type copy of *MPS2* or an empty vector were integrated in single copy into the *LEU2* locus of a *MPS2* deletion covered by a *URA3*-based plasmid containing wild-type *MPS2* (SLJ1901). The ability of each to rescue the *mps2Δ* was tested by plating fivefold serial dilutions of cells on 5-FOA plates (right). As a control, cells were stamped onto SD-URA plates (left). Plates were incubated at 30°C for 2 d. Identical results were obtained at 16, 23, 34, and 37°C (not depicted). (C) Similarly, a nonsense codon was inserted after the indicated amino acid in *MPS2* to generate the C-terminal (Ct) truncation alleles depicted. Mutant genes were transformed into strains containing a deletion of *MPS2* covered by a *URA3*-based plasmid containing wild-type *MPS2* (SLJ1901) plus a *TRP1*-based 2μ plasmid containing nothing (−), *MPS2*, or *MPS3*. The ability of each *mps2* mutant to rescue the deletion in the presence of vector, *MPS2*, and *MPS3* was tested by plating a series of six fivefold dilutions on 5-FOA. After 4 d at 30°C, plates were scored as follows: ++, growth at the fourth dilution; +, growth at the third dilution; +/−, growth at the first and second dilution; −, no growth above background. *mps2-381* cells grew at 23 and 30 but not at 37°C (ts) in the absence of a rescuing plasmid. (D) Mps2 C-terminal deletion mutants were also expressed as MBP fusion proteins in bacteria and mixed with 1 μg purified 6xHis-Mps3SUN. Mps2 fusion proteins were immunoprecipitated using anti-Mps2 antibodies, and the level of each was determined by Western blotting with anti-MBP antibodies (top). Binding to the Mps3 SUN domain was tested by Western blotting with anti-Mps3 antibodies (bottom). (E) *mps2-381* cells (SLJ2006) were transformed with the indicated gene on a 2μ plasmid carrying a *TRP1* marker (pRS424), and the ability of the 2μ plasmid to restore growth to the mutant at 37°C was tested by plating a series of six fivefold dilutions of cells on SD-TRP plates. Plates were incubated for 2 d at 37°C or 3 d at 23°C. (F) The indicated gene on a 2μ *URA3* plasmid (pRS202 or pRS426) was transformed into *mps2-381* cells (SLJ2006) and analyzed for its ability to restore growth at 37°C in a serial dilution assay as described in C. *mps2-381* growth at 37°C was not suppressed by 2μ *SPC42*, 2μ *SPC29*, 2μ *CNM67*, 2μ *NUD1*, 2μ *KAR1*, or 2μ *SFI1*.

(Nishikawa et al., 2003). In contrast, the N terminus of Mps2 is exposed to the cytoplasm/nucleoplasm, whereas the C terminus of Mps2 is in the intermembrane space (Schramm et al., 2000). Therefore, we would predict that the Mps3 SUN domain binds to the C terminus of Mps2. However, neither the Mps2 C terminus nor any other protein sequence in *S. cerevisiae* contain regions of significant similarity to a hidden Markov model of the KASH domain (unpublished data); instead, Mps2 and its orthologues

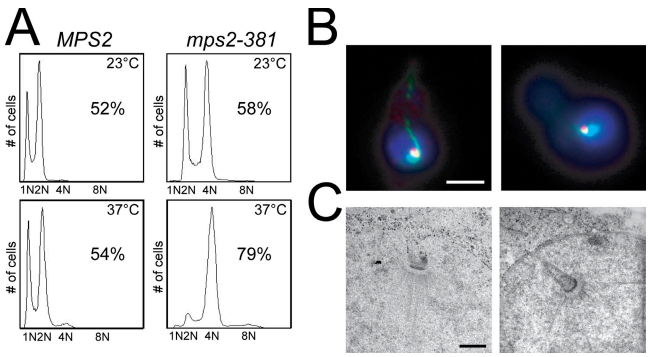

Figure 6. ***mps2-381* mutants are defective in SPB duplication.** (A) Wild-type (SLJ001) and *mps2-381* (SLJ2006) were grown to midlog phase at 23°C and then shifted to 37°C for 4 h. Flow cytometric analysis of DNA content showed that although wild-type cells are haploids (1N and 2N) at 23°C, the *mps2-381* mutants are diploids (2N and 4N) and arrest at 37°C in mitosis. The percentage of large-budded cells was also determined (n = 200). (B) Indirect immunofluorescence microscopy revealed that *mps2-381* cells arrested at 37°C with monopolar spindles: a single microtubule array (anti-Tub1; green) nucleated from one SPB (anti-Tub4; red) associated with one DNA mass (DAPI; blue). Bar, 5 μm. (C) Nuclei from large-budded cells were examined by EM to further analyze SPB number and mitotic spindle structure in *mps2-381* cells arrested at 37°C. Thin section images of two representative SPBs are shown; both SPBs are on deep nuclear invaginations and lack any recognizable half-bridge structure. Bar, 0.2 μm.

from other budding yeasts have a unique C-terminal region that includes seven conserved aromatic residues (Fig. 5 A).

Despite its lack of a KASH domain, the Mps2 C terminus clearly binds to the Mps3 SUN domain in both the gel overlay assay and pull-down assays in vitro (Fig. 4 A and not depicted). In addition, a version of Mps2 lacking the C-terminal amino acids (mps2ΔC; amino acids 1–328) does not bind to the SUN domain in vitro (Fig. 4 A and Fig. 5 D) and *mps2ΔC* is unable to rescue the growth defect of *mps2Δ* and serve as the sole copy of *MPS2* in cells (Fig. 5 B). Thus, the C terminus of Mps2, like the Mps3 SUN domain, is critical for cell viability.

Analysis of a series of point mutations (not depicted) and truncations (Fig. 5 C) in the Mps2 C terminus indicates that residues throughout the region are essential for Mps2 function and for Mps3 binding. Insertion of a nonsense codon after residue 381 in Mps2 resulted in an allele of *MPS2* (*mps2-381*) that encodes a protein containing all but the last six amino acids. The fact that *mps2-381* cells display a conditional growth defect (Fig. 5, C and E), combined with the fact that the mps2-381 protein only weakly bound to the SUN domain in vitro (Fig. 5 D), is evidence that the C terminus of Mps2 is important for the interaction with Mps3 in vivo. Additional support for the notion that the growth defect in *mps2-381* cells is due to loss of Mps3 binding comes from our observations that overexpression of wild-type *MPS3*, but not SUN domain mutants, partially rescues the growth defect of *mps2-381* mutants at 37°C (Fig. 5, E and F). Interestingly, *MPS3* overexpression is unable to suppress *mps2* mutants that contain lesions in the N terminus (not depicted), whereas *BBP1* overexpression, which suppresses some N-terminal *mps2* mutants (Schramm et al., 2000), only weakly rescues growth of *mps2-381* (Fig. 5 F). These results strongly suggest that the SUN domain of Mps3 binds to the C terminus of Mps2 and supports the possibility that loss of

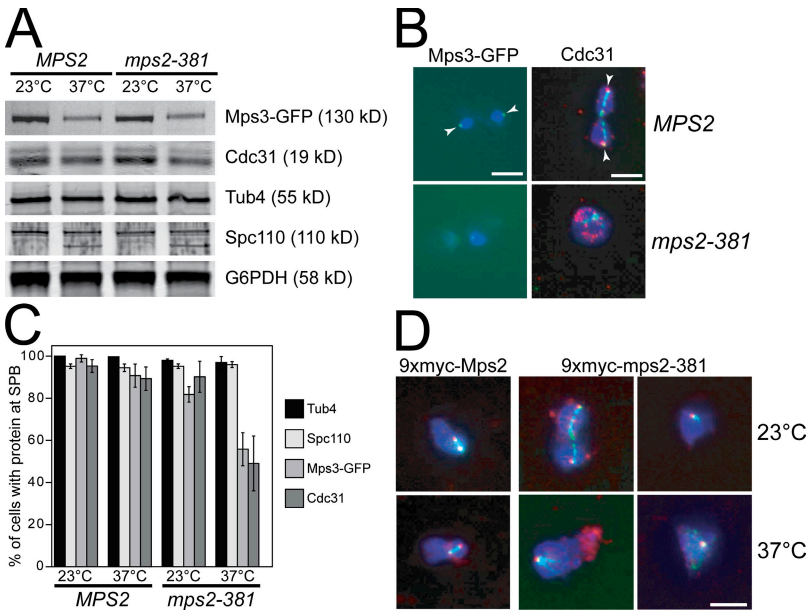

Figure 7. **Mps3 localization to the SPB is compromised in *mps2-381* mutants.** (A) Wild-type (SLJ911) and *mps2-381* (SLJ2056) cells in which the endogenous copy of *MPS3* was replaced with *MPS3-GFP* were grown to midlog phase at 23°C and then shifted to 37°C for 3 h. Levels of Mps3-GFP and other SPB components were analyzed by Western blotting with anti-GFP and other polyclonal antibodies. G6PDH serves as a loading control. (B) Mps3-GFP localization to the SPB was examined by epifluorescence microscopy in wild-type cells (arrowheads; top left), and *mps2-381* mutants (bottom left) that had been shifted to 37°C. Similarly, indirect immunofluorescence microscopy using anti-Cdc31 antibodies (red) was used to compare Cdc31 staining at the SPB at the ends of microtubules (anti-Tub1; green) in wild-type cells (arrowheads; top right) and *mps2-381* mutants (bottom right) at 37°C. In both samples, DNA was visualized by DAPI staining (blue). Bars, 5 μm. (C) Localization of Mps3-GFP and Cdc31 as well as Tub4 and Spc110 was determined in wild-type (SLJ001) and *mps2-381* (SLJ2056) cells grown to midlog phase at 23°C and then shifted to 37°C for 3 h as in B, and the percentage of cells where each protein was clearly observed at the SPB was quantitated. Over 100 cells in two independent experiments were analyzed. (D) Strains containing *9xMYC-MPS2* (SLJ1996) or *9xMYC-mps2-381* (SLJ2139) were grown to midlog phase at 23°C and then shifted to 37°C for 3 h. Indirect immunofluorescence microscopyrevealed that both wild-type 9xMYC-Mps2 and 9xMYC-mps2-381 (9E10 anti-MYC; red) localize to the ends of microtubules (anti-Tub1; green) at both 23 and 37°C and colocalize with the SPB protein Tub4 (not depicted). DNA was visualized by DAPI staining (blue). Because *mps2-381* cells arrest with monopolar spindles, only a single SPB and Mps2 focus is observed at 37°C in the mutant. Bar, 5 μm.

Mps3 binding is responsible for the growth defect of *mps2-381* and other C-terminal Mps2-deletion mutants.

mps2-381 mutants have SPB duplication and karyogamy defects

Asynchronously growing wild-type and *mps2-381* mutant cells were analyzed after a 4-h shift to the nonpermissive temperature (37°C). Flow cytometric analysis of DNA content and budding index confirmed that the *mps2-381* mutants spontaneously diploidize at 23°C and arrest in mitosis at 37°C (Fig. 6 A). Analysis of mitotic spindle morphology by indirect immunofluorescence microscopy and EM revealed that >75% of large-budded *mps2-381* cells contain a monopolar spindle at 37°C (Fig. 6, B and C). Other *mps2* mutants also have monopolar spindles (Winey et al., 1991); however, *mps2-381* mutants have a distinct terminal SPB mutant phenotype: they contain a single monopolar spindle on a deep nuclear invagination, and the SPB appears to have failed to initiate SPB duplication (Fig. 6 C). The morphology of the *mps2-381* SPB is highly reminiscent of many of our *mps3* SUN mutants (Fig. 2 A and Fig. S1), and it appears that *mps2-381* SPBs lack a normal half-bridge, although visualization of the half-bridge by EM alone on such a constricted invagination is difficult. We found no evidence by morphology or by immunolabeling of a second partially assembled SPB like that observed in *mps2-1* mutants in spite of good overall fixation (unpublished data; Winey et al., 1991). This novel terminal SPB phenotype uncovered by the *mps2-381* allele suggests that Mps2 has an earlier function in SPB duplication, perhaps during half-bridge formation or tethering of the half-bridge to the SPB, which was not previously indicated through analysis of other *mps2* mutants.

Like the Mps3 SUN domain, the Mps2 C terminus is important not only for SPB duplication but also for both steps of karyogamy. Although other *mps2-1* alleles also have a mild karyogamy defect, >30% of *mps2-381* cells fail to complete both nuclear congression and fusion, indicating that Mps2–Mps3 binding is important for karyogamy (Fig. 3).

mps2-381 mutants have defects in Mps3 localization

The fact that *mps2-381* mutants have phenotypes very similar to our *mps3* SUN mutants and to other mutants that lack a functional half-bridge led us to examine the localization and levels of Mps3 and the half-bridge component Cdc31 in *mps2-381* cells. Asynchronously growing wild-type and *mps2-381* cells that have the endogenous copy of *MPS3* fused to GFP were shifted to 37°C for 3 h. Western blot analysis revealed that Mps3-GFP, as well as other SPB components such as Cdc31, Spc110, and Tub4, were expressed at similar levels in *MPS2* and *mps2-381* cells (Fig. 7 A). However, we consistently saw a decrease in the number of *mps2-381* cells grown at 37°C containing Mps3-GFP, as well as a decrease in the overall intensity of Mps3-GFP epifluorescence at the SPB (Fig. 7, B and C). Cdc31 staining at the SPB by indirect immunofluorescence also decreased in *mps2-381* mutants at 37°C (Fig. 7, B and C). Instead of a distinct SPB signal, Mps3-GFP was diffusely localized and Cdc31 appeared as punctate spots in *mps2-381* cells at 37°C. No change in expression or localization of core SPB components such as Spc110 and Tub4 was observed in *mps2-381* mutants at either temperature (Fig. 6 B and Fig. 7 C). The failure of *mps2-381* mutants to localize Mps3-GFP and Cdc31 to the SPB is not due to defects in 9xMYC-mps2-381 expression or its localization to the SPB; 9xMYC-Mps2 and 9xMYC-mps2-381 both localized to the SPB at 23 and 37°C (Fig. 7 D). Together with our data showing that mps2-381 binding to the

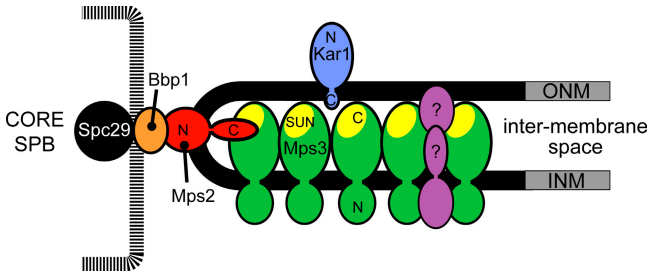

Figure 8. **Binding of the Mps3 SUN domain to Mps2 C terminus tethers the SPB to the half-bridge.** Mps3 (green) is an integral membrane protein localized primarily to the inner nuclear membrane with its N terminus exposed to the nucleoplasm/cytoplasm and its C terminus located in the membrane space between the inner and outer nuclear membranes (INM and ONM, respectively). Here, the SUN domain of Mps3 (yellow) can interact with the C terminus of integral membrane proteins such as Mps2 (red) to build the half-bridge (black) and anchor it to the core SPB, which is important for SPB duplication and karyogamy. Previous work showed that the N terminus of Mps2 binds to the soluble protein Bbp1 (orange), which interacts with the core SPB protein Spc29 (black; Schramm et al., 2000). It is possible that the SUN domain of Mps3 also interacts with other proteins, such as Jem1 (purple; see Discussion).

Mps3 SUN domain is reduced in vitro, these data strongly suggest that *mps2-381* mutants fail to bind and localize components of the half-bridge to the SPB. We propose that the Mps3 SUN domain and the Mps2 C terminus form an intermolecular bridge spanning the nuclear membranes to tether the half-bridge to the core SPB. This interaction is critical for assembly and/or maintenance of an intact half-bridge (Fig. 8).

Discussion

Association between the core SPB and the half-bridge is critical for SPB duplication and function, yet the molecular details of this link have not been characterized at a biochemical level. In this work, we show that SPBs in Mps3 SUN domain and Mps2 C-terminal mutants lack an associated half-bridge and find that the Mps2 C terminus directly binds to Mps3 in a SUN domain–dependent manner. This strongly suggests that the Mps2–Mps3 interaction is essential to anchoring the half-bridge to the core SPB (Fig. 8). When combined with previous studies showing that the N terminus of Mps2 binds to Bbp1, which in turn interacts with the central plaque component Spc29 (Schramm et al., 2000), our results provide a missing physical connection between the half-bridge and the core SPB.

Previous analysis of *mps2-1* mutants showed that Mps2 function is required for insertion of the newly duplicated SPB into the nuclear envelope (Winey et al., 1991). However, our findings that *mps2-381* mutants lack any recognizable half-bridge structure and fail to localize Mps3 and Cdc31 to the SPB suggests that Mps2 has an additional function earlier in SPB duplication. Based on analysis of Mps2–Mps3 binding, we propose that Mps3 recruits and binds to Mps2 at the distal tip of the newly assembled bridge during SPB duplication. Once this connection between the C terminus of Mps2 and the Mps3 SUN domain is established, Mps2 can interact through its N terminus with additional proteins such as Bbp1, Nbp1, and Ndc1 to facilitate insertion of the newly duplicated SPB into the nuclear envelope. This model would explain why previously characterized *mps2* alleles, which all contain N-terminal mutations, fail in the late step of SPB duplication like *bbp1-1*, *nbp1-td*, and *ndc1-1* mutants (Winey et al., 1991, 1993; Schramm et al., 2000; Araki et al., 2006). We would also predict that binding between Mps2 and Mps3 is required to tether the half-bridge to the core SPB from the point of SPB duplication throughout the rest of the cell cycle. Consistent with this hypothesis, *mps2-381* cells fail to maintain an intact half-bridge at the restrictive temperature, resulting in defects in the earliest step of SPB duplication as well as in karyogamy.

Is the Mps2–Mps3 interaction the only binding event required to tether the half-bridge to the core SPB? Two-hybrid interactions have been observed between Bbp1 and Kar1 (Schramm et al., 2000) as well as between Ndc1 and Kar1 (unpublished data), and numerous genetic interactions have been reported among Mps2, Ndc1, Bbp1, Nbp1, and components of the half-bridge (Schramm et al., 2000; Jaspersen et al., 2002; Araki et al., 2006), so we suspect that a complex set of protein–protein interactions likely anchors the half-bridge to the core SPB. Multiple overlapping interactions would help ensure the integrity of the entire SPB and allow it to withstand microtubule forces that push and pull on the SPB and nucleus during the yeast life cycle. Redundancy in protein–protein interactions holding the half-bridge to the core SPB could also explain why we observe only ~50% reduction in Mps3 and Cdc31 localization to the SPB in *mps2-381* mutants at 37°C. Further analysis of the molecular interactions between the membrane and half-bridge components of the SPB will allow us to better understand how the SPB is assembled and duplicated.

Analysis of Mps3 SUN mutants in yeast suggest that SUN proteins have multiple evolutionarily conserved functions. First, the role of the Mps3 SUN domain in maintaining SPB integrity by tethering the soluble core proteins to the nuclear envelope components suggests the interesting possibility that this protein family is involved in connecting centrosomes to the nuclear envelope. Although the idea that centrosomes are physically linked to the nuclear envelope is controversial, old and new evidence suggests that such an association may exist (Bornens, 1977; Nadezhdina et al., 1979; Kuriyama and Borisy, 1981; Malone et al., 2003). Low sequence conservation between SUN domains makes it impossible to predict the phylogenetic relationships of most proteins within the SUN family with statistical significance. However, our functional data suggests that Mps3 is most related to fission yeast Sad1, *C. elegans* SUN-1, and mammalian Spag4, which have been shown to be essential for tethering SPBs, centrosomes, and axonemes, respectively, with the nuclear envelope (Hagan and Yanagida, 1995; Shao et al., 1999; Malone et al., 2003). Interestingly, these Mps3-like SUN proteins not only interact with various types of microtubule-organizing centers but also appear to bind to proteins, such as Kms1, ZYG-12, and now Mps2, that show very little sequence similarity to the KASH domain of other SUN binding proteins that interact with the actin cytoskeleton (Starr and Fischer, 2005). One idea is that microtubule SUN proteins may recognize a distinct or divergent motif that is currently poorly defined because of the low number of known binding proteins.

The requirement of an intact Mps3 SUN domain for nuclear migration during karyogamy is consistent with the role of *C. elegans* UNC-84 and SUN-1 in nuclear positioning (Malone et al., 1999, 2003). Mps3 SUN mutants also affect the second step of karyogamy. This may be due to a defect in SPB integrity; however, given that hSun1 is required for homotypic membrane fusion in vitro (Hoffenberg et al., 2000), the requirement for Mps3 during nuclear fusion may reflect a more general role for SUN proteins as mediators of membrane fusion. Interestingly, the SUN domain region of Mps3 has been shown to interact with the DnaJ-like ER membrane chaperone Jem1, which is required for membrane fusion after mating (Nishikawa et al., 2003).

SUN proteins also appear to have functions within the nucleus. Sad1 is required for formation of the meiotic bouquet during fission yeast meiosis (Shimanuki et al., 1997; Chikashige et al., 2006), and mammalian Sun1 proteins have Zn^{2+} finger domains that may interact directly with chromatin (Haque et al., 2006). In addition, Mps3 is required for the establishment of sister chromatid cohesion during S phase in budding yeast (Antoniacci et al., 2004), and one of our SUN domain mutants (*mps3-Y502H*) is found in the *mps3-5* allele that has defects in both centromere and telomere cohesion (Antoniacci and Skibbens, 2006). Additional nuclear functions could be one reason for the spindle checkpoint–dependent mitotic delay that we observed in *mps3-W477A*, *-F592S*, and *-ΔSUN2* cells (unpublished data). How mutations in the SUN domain might affect nuclear functions of Mps3 is unclear at present. However, our identification of Mps3 as the budding yeast SUN protein should facilitate rapid identification and analysis of additional SUN binding partners and greatly enhance our understanding of SUN protein functions.

Materials and methods

Yeast strains and plasmids

All strains are derivatives of W303 (*ade2-1 trp1-1 leu2-3,112 ura3-1 his3-11,15 can1-100*) and are listed in Table S1 (available at http://www.jcb.org/cgi/content/full/jcb.200601062/DC1). The entire ORF of *MPS2* or *MPS3* was deleted in a diploid with *HIS3MX6* or *KANMX6* using PCR-based methods, and the strain was transformed with a centromeric *URA3*-marked plasmid containing the corresponding wild-type ORF, sporulated, and dissected to generate *mps2Δ::KANMX6 pURA3-MPS2* and *mps3Δ::HIS3MX6 pURA3-MPS3* strains in both mating types. *mps2* and *mps3* alleles in pRS305 were created by oligonucleotide-directed mutagenesis and integrated into the *LEU2* locus in single copy in the appropriate deletion. *MPS3* was fused to 3xFLAG and *MPS2* was fused to 13xMYC using PCR. The *9xMYC-mps2-381* was created by mutagenesis of *pRS304-9xMYC-MPS2* (Munoz-Centeno et al., 1999), and vectors containing both wild-type and mutant forms of *MPS2* were cut with BstZ17I to direct integration into the *TRP1* locus of SLJ1901 followed by loss of the covering *MPS2* plasmid on plates containing 5-fluoorotic acid (5-FOA).

SAD1 and *MPS3* were amplified by PCR from pREP42-*SAD1* (a gift from I. Hagan, Paterson Institute for Cancer Research, Manchester, UK) and pSJ140 (Jaspersen et al., 2002), respectively, and cloned into a pRS306-based vector containing the *GAL1/10* promoter to create *pURA3-GAL-SAD1* (pSJ379) and *pURA3-GAL-MPS3* (pSJ146). *MPS2* and mutants, the SUN domain of *MPS3* and mutants and *SPC29* were amplified by PCR and cloned into pMAL-c2 (New England Biolabs, Inc.) or pQE10/pQE11 (QIAGEN) for expression in bacteria as MBP or 6xHis fusion proteins, respectively.

Protein techniques

6xHis-Spc29 was purified from BL21(DE3) bacteria transformed with pQE11-*SPC29* (pSJ260) by metal affinity followed by anion exchange chromatography, and the C terminus of Mps3 was purified from BL21(DE3) pLysS bacteria transformed with pMALc2-*MPS3-Ct* (pSJ151) using amylose resin. Antibodies against purified 6xHis-Spc29 or MBP-Mps3-Ct were generated in rabbits (Animal Pharm) and purified according to the manufacturer's instructions on a Spc29 or Mps3 column created using the Sulfo-link kit (Pierce Chemical Co.). Mps2 antibodies were generated by injecting a KLH-coupled peptide corresponding to residues 212–233 of Mps2 into guinea pigs (Pocono) followed by affinity purification on MBP-Mps2 bound to nitrocellulose filters.

The Mps3 SUN domain was also purified from BL21(DE3) pLysS bacteria transformed with pQE10-*mps3SUN* (pSJ413) by metal affinity chromatography, and 0.5 mg purified 6xHis-mps3SUN labeled with Alexa 680 as described previously (Jaspersen et al., 2002). Expression of MBP, MBP-Mps2 (pSJ426), and MBP-Kar1 (pSJ425) in BL21(DE3) pLysS cells was induced by the addition of 0.1 mM IPTG for 2 h at 23°C. Cells from 1 ml of culture were resuspended in 200 μl 2× SDS sample buffer and heated to 100°C for 5 min, 5 μl of MBP-Mps2 and MBP-Kar1 and 2 μl of MBP-only samples were separated by 8% SDS-PAGE, and proteins were electrophoretically transferred to nitrocellulose. Membranes were probed with 10 μg Alexa 680–labeled 6xHis-mps3SUN, and binding was assessed using the Odyssey imaging system (LiCor). Expression of bacterial proteins was confirmed by Western blotting with a 1:1,000 dilution of anti-MBP antibodies (New England Biolabs, Inc.). For bacterial pull-down assays, MBP, MBP-Mps2, and MBP-mps2 mutants were expressed in BL21(DE3) pLysS cells by the addition of 0.1 mM IPTG for 2 h at 23°C and cell pellets from 2 ml of culture were resuspended in 0.5 ml PBS containing 0.1% Triton X-100 and 1 mM PMSF, vortexed for 5 min at 4°C, and centrifuged at 14,000 *g* for 10 min at 4°C. 100 μl of each extract was mixed with 1 μg of purified 6xHis-mps3SUN in a 500-μl immunoprecipitation that included 2 μl protein A–coated magnetic beads (Dynal) and 1 μl of affinity-purified anti-Mps2 antibodies. After a 1-h incubation a 4°C, immunoprecipitates were washed five times in PBS containing 0.1% Triton X-100 and an additional 250 mM NaCl.

Spheroplast lysates were prepared from 100 OD_{600} midlog phase cells. Harvested cells were resuspended in 5 ml spheroplast buffer (50 mM Tris-HCl, pH 7.5, 1.2 M sorbitol, and 10 mM NaN_3) containing 40 mM β-mercaptoethanol and treated with 300 μg/ml zymolase 100T for 30 min at 30°C. Cells were then washed three times in spheroplast buffer, resuspended in 2.5 ml spheroplast lysis buffer (20 mM Hepes-KOH, pH 7.4, 100 mM K-acetate, 5 mM Mg-acetate, 1 mM EDTA, 1 mM PMSF, and 1 μg/ml each of pepstatin A, aprotinin, and leupeptin), and lysed by dounce homogenization. Lysates were transferred to ice and treated with 0.2 mg/ml dithiobis(succinimidyl)propionate for 10 min. Cross-linking was quenched by addition of 50 mM Tris-HCl, pH 8.0, and lysates were centrifuged at 13,000 *g* for 15 min at 4°C. The pellet was resuspended in 2.5 ml solubilization buffer (spheroplast lysis buffer plus 1 M NaCl and 1% Triton X-100) and recentrifuged at 13,000 *g* for 15 min at 4°C. The supernatant was added to 20 ml spheroplast lysis buffer immediately before immunoprecipitation.

Ground lysates were prepared from 500 OD_{600} of midlog phase cells as described previously (Niepel et al., 2005). In brief, cells were frozen in liquid nitrogen and ground with a Retsch ball mill. Ground cell powder was allowed to thaw on ice and resuspended in 10 ml extraction buffer (25 mM Hepes-NaOH, pH 7.5, 300 mM NaCl, 0.1 mM EDTA, 0.5 mM EGTA, 2 mM $MgCl_2$, 0.5% Triton X-100, 1 mM DTT, 1 mM PMSF, and 1 μg/ml each of pepstatin A, aprotinin, and leupeptin). After homogenization with a Polytron 10/35 for 30 s, lysates were centrifuged at 3,000 *g* for 10 min at 4°C, and the resulting supernatant was used for immunoprecipitations.

100 μl FLAG M2 (Sigma-Aldrich) or 9E10 conjugated (Santa Cruz Biotechnology, Inc.) beads were added to lysates to immunoprecipitate Mps3-FLAG or Mps2-13xMYC, respectively. After a 2-h incubation at 4°C, beads were washed five times in extraction buffer, and 1/10 of the bound protein and 1/1,000 of the input protein was analyzed by SDS-PAGE followed by Western blotting. The following primary antibody dilutions were used: 1:5,000 anti-MYC A14 (Santa Cruz Biotechnology, Inc.), 1:1,000 anti-FLAG (Sigma-Aldrich), 1:2,000 anti-Cdc31 (Jaspersen et al., 2002), 1:5,000 anti-Spc29, 1:2,000 anti-Mps3, 1:2,000 anti-Spc110 (a gift of T. Davis, University of Washington, Seattle, WA), 1:1,000 anti-GFP B34 (Covance), 1:2,500 anti-MBP (New England Biolabs, Inc.), and 1:10,000 anti–glucose-6-phosphate dehydrogenase (G6PDH; Sigma-Aldrich). Alkaline phosphatase–conjugated secondary antibodies were used at 1:10,000 (Promega).

Karyogamy assay

Approximately 5×10^6 midlog phase cells of opposite mating types grown at 23°C were mixed onto a 45-μm nitrocellulose filter, and filters were

incubated on YPD plates for 5 h at 30°C. Cells were then stained with DAPI, and nuclear position was analyzed by fluorescence microscopy.

Cytological techniques

Analysis of DNA content by flow cytometry, EM, and protein localization by indirect immunofluorescence and epifluorescence microscopy were performed as previously described (Jaspersen et al., 2002). Spc110 polyclonal antibodies were a gift from T. Davis and were used at a 1:2,000 dilution. Mps3 was localized using affinity-purified anti-Mps3 antibodies diluted 1:500 in PBS containing 3% BSA and 0.1% NP-40 followed by detection with Alexa 555–conjugated goat anti–rabbit secondary antibodies (Invitrogen) diluted 1:20,000 in the same buffer. Cells were examined with an Axioimager (Carl Zeiss MicroImaging, Inc.) using a 100× Plan-Fluar lens (NA = 1.45; Carl Zeiss MicroImaging, Inc.), and images were captured with a digital camera (Orca ER; Hamamatsu) and processed using Axiovision 4.0 (Carl Zeiss MicroImaging, Inc.).

Sequence analysis

Homologues of Mps3 were detected through iterative searches of the nonredundant protein sequence database (National Center for Biotechnology Information) using the PSI-BLAST program (Altschul et al., 1997). Sequences corresponding to the SUN domain of Mps3 homologues and C termini of putative SUN binding proteins were aligned using ClustalW, and phylogenetic analysis was performed using the MEGA3 software.

Online supplemental material

Fig. S1 shows that ts SUN domain mutants arrest in mitosis because of a defect in SPB duplication. Fig. S2 shows a phylogenetic analysis of SUN domains. Table S1 lists yeast strains. Table S2 shows SUN domain mutants. Table S3 gives copy number–dependent SUN domain mutants. Online supplemental material is available at http://www.jcb.org/cgi/content/full/jcb.200601062/DC1.

We thank I. Hagan and T. Davis for reagents; K. Delventhal, J. Wunderlich, and J. Schwartz for technical assistance; and D. Starr, J. Gerton, K. Lee, C. Pearson, and S. Hawley for valuable discussions and comments on the manuscript. We are especially grateful to S. Shelton, J. Bupp, and E. Hoffman for their contributions to this project.

This work was supported by funding from the National Institutes of General Medical Sciences (grant GM51312 to M. Winey) and the Leukemia and Lymphoma Society (to S.L. Jaspersen). S.L. Jaspersen and A. Mushegian are also funded by the Stowers Institute for Medical Research.

Submitted: 12 January 2006
Accepted: 21 July 2006

References

Altschul, S.F., T.L. Madden, A.A. Schaffer, J. Zhang, Z. Zhang, W. Miller, and D.J. Lipman. 1997. Gapped BLAST and PSI-BLAST: a new generation of protein database search programs. *Nucleic Acids Res.* 25:3389–3402.

Antoniacci, L.M., and R.V. Skibbens. 2006. Sister-chromatid telomere cohesion is nonredundant and resists both spindle forces and telomere motility. *Curr. Biol.* 16:902–906.

Antoniacci, L.M., M.A. Kenna, P. Uetz, S. Fields, and R.V. Skibbens. 2004. The spindle pole body assembly component Mps3p/Nep98p functions in sister chromatid cohesion. *J. Biol. Chem.* 279:49542–49550.

Araki, Y., C.K. Lau, H. Maekawa, S.L. Jaspersen, T.H. Jr. Giddings, E. Schiebel, and M. Winey. 2006. The *Saccharomyces cerevisiae* spindle pole body (SPB) component Nbp1p is required for SPB membrane insertion and interacts with the integral membrane proteins Ndc1p and Mps2p. *Mol. Biol. Cell.* 17:1959–1970.

Bornens, M. 1977. Is the centriole bound to the nuclear membrane? *Nature.* 270:80–82.

Byers, B., and L. Goetsch. 1974. Duplication of spindle plaques and integration of the yeast cell cycle. *Cold Spring Harb. Symp. Quant. Biol.* 38:123–131.

Byers, B., and L. Goetsch. 1975. Behavior of spindles and spindle plaques in the cell cycle and conjugation of *Saccharomyces cerevisiae*. *J. Bacteriol.* 124:511–523.

Chikashige, Y., C. Tsutsumi, M. Yamane, K. Okamasa, T. Haraguchi, and Y. Hiraoka. 2006. Meiotic proteins Bqt1 and Bqt2 tether telomeres to form the bouquet arrangement of chromosomes. *Cell.* 125:59–69.

Cliften, P., P. Sudarsanam, A. Desikan, L. Fulton, B. Fulton, J. Majors, R. Waterson, B.A. Cohen, and M. Johnston. 2003. Finding functional features in *Saccharomyces* genomes by phylogenetic footprinting. *Science.* 301:71–76.

Hagan, I., and M. Yanagida. 1995. The product of the spindle formation gene *sad1+* associates with the fission yeast spindle pole body and is essential for viability. *J. Cell Biol.* 129:1033–1047.

Haque, F., D.J. Lloyd, D.T. Smallwood, C.L. Dent, C.M. Shanahan, A.M. Fry, R.C. Trembath, and S. Shackleton. 2006. SUN1 interacts with nuclear lamin A and cytoplasmic nesprins to provide a physical connection between the nuclear lamina and the cytoskeleton. *Mol. Cell. Biol.* 26:3738–3751.

Hoffenberg, S., X. Liu, L. Nikolova, H.S. Hall, W. Dai, R.E. Baughn, B.F. Dickey, M.A. Barbieri, A. Aballay, P.D. Stahl, and B.J. Knoll. 2000. A novel membrane-anchored Rab5 interacting protein required for homotypic endosome fusion. *J. Biol. Chem.* 275:24661–24669.

Jaspersen, S.L., and M. Winey. 2004. The budding yeast spindle pole body: structure, duplication, and function. *Annu. Rev. Cell Dev. Biol.* 20:1–28.

Jaspersen, S.L., T.H. Giddings Jr., and M. Winey. 2002. Mps3p is a novel component of the yeast spindle pole body that interacts with the yeast centrin homologue Cdc31p. *J. Cell Biol.* 159:945–956.

Kilmartin, J.V. 2003. Sfi1p has conserved centrin-binding sites and an essential function in budding yeast spindle pole body duplication. *J. Cell Biol.* 162:1211–1221.

Kuriyama, R., and G.G. Borisy. 1981. Centriole cycle in Chinese hamster ovary cells as determined by whole-mount electron microscopy. *J. Cell Biol.* 91:814–821.

Li, S., A.M. Sandercock, P. Conduit, C.V. Robinson, R.L. Williams, and J.V. Kilmartin. 2006. Structural role of Sfi1p-centrin filaments in budding yeast spindle pole body duplication. *J. Cell Biol.* 173:867–877.

Malone, C.J., W.D. Fixsen, H.R. Horvitz, and M. Han. 1999. UNC-84 localizes to the nuclear envelope and is required for nuclear migration and anchoring during *C. elegans* development. *Development.* 126:3171–3181.

Malone, C.J., L. Misner, N. Le Bot, M. Tsai, J.M. Campbell, J. Ahringer, and J.G. White. 2003. The *C. elegans* hook protein, ZYG-12, mediates the essential attachment between the centrosome and nucleus. *Cell.* 115:825–836.

Mans, B.J., V. Anantharaman, L. Aravind, and E.V. Koonin. 2004. Comparative genomics, evolution and origins of the nuclear envelope and nuclear pore complex. *Cell Cycle.* 3:1612–1637.

Munoz-Centeno, M.C., S. McBratney, A. Monterrosa, B. Byers, C. Mann, and M. Winey. 1999. *Saccharomyces cerevisiae MPS2* encodes a membrane protein localized at the spindle pole body and the nuclear envelope. *Mol. Biol. Cell.* 10:2393–2406.

Nadezhdina, E.S., D. Fais, and Y.S. Chentsov. 1979. On the association of centrioles with the interphase nucleus. *Eur. J. Cell Biol.* 19:109–115.

Niepel, M., C. Strambio-de-Castillia, J. Fasolo, B.T. Chait, and M.P. Rout. 2005. The nuclear pore complex-associated protein, Mlp2p, binds to the yeast spindle pole body and promotes its efficient assembly. *J. Cell Biol.* 170:225–235.

Nishikawa, S., Y. Terazawa, T. Nakayama, A. Hirata, T. Makio, and T. Endo. 2003. Nep98p is a component of the yeast spindle pole body and essential for nuclear division and fusion. *J. Biol. Chem.* 278:9938–9943.

Rose, M.D. 1996. Nuclear fusion is the yeast *Saccharomyces cerevisiae*. *Annu. Rev. Cell Dev. Biol.* 12:663–695.

Rose, M., and G. Fink. 1987. *KAR1*, a gene required for function of both intranuclear and extranuclear microtubules in yeast. *Cell.* 48:1047–1060.

Schramm, C., S. Elliott, A. Shevchenko, and E. Schiebel. 2000. The Bbp1-Mps2 complex connects the SPB to the nuclear envelope and is essential for SPB duplication. *EMBO J.* 19:421–433.

Shao, X., H.A. Tarnasky, J.P. Lee, R. Oko, and F.A. van der Hoorn. 1999. Spag4, a novel sperm protein, binds outer dense-fiber protein Odf1 and localizes to microtubules of manchette and axoneme. *Dev. Biol.* 211:109–123.

Shimanuki, M., F. Miki, D.Q. Ding, Y. Chikashige, Y. Hiraoka, T. Horio, and O. Niwa. 1997. A novel fission yeast gene, *kms1+*, is required for the formation of meiotic prophase-specific nuclear architecture. *Mol. Gen. Genet.* 254:238–249.

Spang, A., I. Courtney, U. Fackler, M. Matzner, and E. Schiebel. 1993. The calcium-binding protein cell division cycle 31 of *Saccharomyces cerevisiae* is a component of the half bridge of the spindle pole body. *J. Cell Biol.* 123:405–416.

Spang, A., I. Courtney, K. Grein, M. Matzner, and E. Schiebel. 1995. The Cdc31-binding protein Kar1p is a component of the half bridge of the yeast spindle pole body. *J. Cell Biol.* 128:863–877.

Starr, D.A., and J.A. Fischer. 2005. KASH 'n Karry: the KASH domain family of cargo-specific cytoskeletal adaptor proteins. *Bioessays.* 27:1136–1146.

Vallen, E.A., T.Y. Scherson, T. Roberts, K. van Zee, and M.D. Rose. 1992. Asymmetric mitotic segregation of the yeast spindle pole body. *Cell.* 69:505–515.

Vallen, E., W. Ho, M. Winey, and M. Rose. 1994. Genetic interactions between *CDC31* and *KAR1*, two genes required for duplication of the microtubule organizing center in *Saccharomyces cerevisiae*. *Genetics.* 137:407–422.

Winey, M., L. Goetsch, P. Baum, and B. Byers. 1991. *MPS1* and *MPS2*: novel yeast genes defining distinct steps of spindle pole body duplication. *J. Cell Biol.* 114:745–754.

Winey, M., M.A. Hoyt, C. Chan, L. Goetsch, D. Botstein, and B. Byers. 1993. *NDC1*: a nuclear periphery component required for yeast spindle pole body duplication. *J. Cell Biol.* 122:743–751.